The Fast Multipole Boundary Element Method for plane anisotropic problems

Dias Júnior,A.B

Albuquerque,E.L

afonso.enm@gmail.com

eder@unb.br

Universidade of Brasília - Departamento do Engenharia Mecânica

Darcy Ribeiro Campus, 70910-900, Brasília, Brazil,

Abstract. *This paper presents a Fast Multipole Boundary Element Method (FMBEM) for large-scale analysis of plane anisotropic problems. Integral equations for plane anisotropic problems are written in a complex form. Fundamental solutions are expanded into Taylor series and the integration on far elements are written considering only locations of element and expansion point (location of the source point has no influence on far element integration). A hierarchical tree structure is assembled in order to group near and far elements. Integration of near elements is treated by the direct application of the boundary element method while fast multipole expansion is used for integration of far element. A numerical example is presented to study the behaviour of fast multipole BEM formulation for different numbers of elements per cell.*

Keywords: *Fast Multipole, Boundary Element Method, Anisotropic elasticity*

1 INTRODUCTION

Boundary Element Method (BEM) is a computational method highly recognized for solving many problems in different research fields, such as fracture mechanics, wave propagation, fluid flows, geomechanics and heat transfer. Although it is very effective for modeling and meshing problems, it is not efficient to solve problems with few thousands of DOFs (degrees of freedom). This method produces dense and nonsymmetrical matrices that require $O(N^2)$ operations to compute their coefficients and $O(N^3)$ operations to solve the system of equations by direct solvers Liu (2009), being N the number of DOFs of the model. This issue has prevented spread of BEM to solve large scale problems.

A way to overcome this drawback is to accelerate BEM with Fast Multipole Method (FMM), proposed by Greengard and Rokhlin (1987). The FMM increases performance of BEM, decreasing CPU time and memory used for storing the coefficients of the matrices and to solve the system of equation. The FMM decreases the complexity of the problem to O(N) because it accelerates matrix-vector multiplication created by iterative methods. In this article generalized minimum residual method (GMRES) was selected as iterative solver, because preconditioned Kyrlov subspace methods are well-effective to solve large scale linear systems Zejun C. (2010). Furthermore, the matrix-vector is split into two parts in the FMM algorithm Hafla (2005). We have the near-field part and the far-field part. The first part is composed of elements that are close to source point and the second part by elements that are distant to source point. These divisions of elements in near-field and far-field are created by the tree-structure. For elements in the far-field fast BEM is applied, and for elements in the near-field conventional BEM is used. Another feature of FMM does not form the entire matrix during matrix-vector multiplication for the far field part. This increases the performance of the method.

Application of fast multipole BEM was investigated by many authors, including Peirce (1995) for 2D elastostatics, Popov (2001) for 3D elastostatics, Yoshida (2001a,b) for 3D elastostatic crack problems, Liu (2005) for carbon-nanotube composites, Wang (2005, 2004) to simulate composite materials, Wang (2006) to analyze fatigue crack growth and a review of fast multipole BEM was presented by Nishimura (2002). In this paper, we will present a fast multipole BEM formulation for 2D anisotropic elasticity problems. First of all, the anisotropic fundamental solutions are expanded by Taylor series, doing Multipole Expansion (*Moments*). These expansions are made in complex variables because they are more efficient than expansion in real variables Liu (2008). After, the operations *Moment to Moment* (M2M), *Local expansion*, *Moment to Local* (M2L), *Local to Local* (L2L) are introduced to evaluate the integrals of the BEM. A hierarchical tree structure is assembled in order to group near and far elements from the element that contain source point. Integration of near elements is treated by direct application of BEM while fast multipole BEM is used for integration of far elements. For elements considered far from a source point, FMM changes element-to-element interactions to cell-to-cell interactions, because tree structure and the operations mentioned above are responsible for change in these interactions Liu (2009). Numerical examples are presented to study the accuracy and efficiency of the fast multipole BEM formulation to solve anisotropic elasticity problems. These results will strengthen the potential of this method to solve large-scale problems.

2 FUNDAMENTAL SOLUTIONS

The two fundamental solutions used for anisotropic problems in this paper are:

$$U_{ji}(\mathbf{z}, \mathbf{z_o}) = 2Re[q_{i1}\Phi_1 + q_{i2}\Phi_2] = 2Re[q_{i1}A_{j1}\ln(z_{o1} - z_1) + q_{i2}A_{j2}\ln(z_{o2} - z_2)] \tag{1}$$

and:

$$T_{ij}(\mathbf{z}, \mathbf{z_o}) = 2Re\left[\frac{g_{j1}(\mu_1 n_1 - n_2)A_{i1}}{(z_{o1} - z_1)} + \frac{g_{j2}(\mu_2 n_1 - n_1)A_{i2}}{(z_{o2} - z_2)}\right] \tag{2}$$

where Eq. (1) and (2) represent the fundamental solutions for displacement and traction, respectively. The terms (μ_k, q_{ik}, g_{jk} and A_{ik}) are material complex constants and their numerical values are presented in Table 1. The field point is represented by (z) field point and the source point by (z_o). They are written in complex notation as:

$$\mathbf{z} = \left\{ \begin{array}{c} z_1 \\ z_2 \end{array} \right\} = \left\{ \begin{array}{c} x_1 + \mu_1 x_2 \\ x_1 + \mu_2 x_2 \end{array} \right\} \tag{3}$$

$$\mathbf{z} = \left\{ \begin{array}{c} z_{o1} \\ z_{o2} \end{array} \right\} = \left\{ \begin{array}{c} x_{o1} + \mu_1 x_{o2} \\ x_{o1} + \mu_2 x_{o2} \end{array} \right\} \tag{4}$$

The material complex constants are calculated by the following equations:

$$a_{11}\mu^4 - 2a_{16}\mu^3 + (2a_{12} + a_{66})\mu^2 - 2a_{26}\mu + a_{22} = 0, \tag{5}$$

$$q_{ik} = \left[\begin{array}{c} a_{11}\mu_k^2 + a_{12} - a_{16}\mu_k \\ a_{12}\mu_k + a_{22}/\mu_k - a_{26} \end{array} \right] \tag{6}$$

$$g_{jk} = \left[\begin{array}{cc} \mu_1 & \mu_2 \\ -1 & -1 \end{array} \right] \tag{7}$$

$$\left[\begin{array}{cccc} 1 & -1 & 1 & -1 \\ \mu_1 & -\overline{\mu}_1 & \mu_2 & -\overline{\mu}_2 \\ q_{11} & -\overline{q}_{11} & q_{12} & -\overline{q}_{12} \\ q_{21} & -\overline{q}_{21} & q_{22} & -\overline{q}_{22} \end{array} \right] \left\{ \begin{array}{c} A_{j1} \\ \overline{A}_{j1} \\ A_{j2} \\ \overline{A}_{j2} \end{array} \right\} = \left\{ \begin{array}{c} \delta_{j2}/(2\pi i) \\ -\delta_{j1}/(2\pi i) \\ 0 \\ 0 \end{array} \right\} \tag{8}$$

Table 1: The values of material complex constants.

	μ_i	i and j	A_{ij}	q_{ij}	g_{ij}
1	-0.1623 + 0.8860i 11	11	0.0431 - 02301i	-0.1411 - 0.0276i	-0.1623 + 0.8860i
2	0.1446 + 0.8440i	12	0.0264 + 0.2301i	-0.1329 + 0.0263i	0.1146 + 0.8440i
	——	21	0.1969 - 0.0041i	-0.0015 - 0.1209i	-1.000
	——	22	-0.1972 - 0.0755i	0.069 - 01233i	-1.000

being a_{11}, a_{12}, a_{16}, a_{22}, a_{26} and a_{66} the coefficients of elastic compliance and the proof of the Eq.(7) and Eq.(8) can be found in Sollero (1994) and Albuquerque (2001).

3 Fast Multipole Method for Anisotropic Problems

The main procedures to implement the FMM for anisotropic problems are presented in this section. First of all, we expand the fundamental solutions in Taylor series. Following it, we will describe the operations applied by FMM. So, to expand Eq.(1) and Eq.(2) in Taylor series, consider the following function and its derivatives:

$$G(z_o, z) = \log(z_o - z) \tag{9}$$

$$G^{'}(z_o, z) = \frac{\partial G(z_o, z)}{\partial z} = \frac{1}{(z - z_o)} \tag{10}$$

Now, we are rewriting the fundamental solutions with Eq.(9) and Eq. (10) as:

$$U_{ij}(z_o, z) = 2Re\left[q_{i1}A_{j1}G(z_{o_1}, z_1) + q_{i2}A_{j2}G(z_{2o}, z_2)\right] \tag{11}$$

$$T_{ij}(z_o, z) = 2Re\left[G^{'}(z_{1o}, z_1)g_{i1}(\mu_1 n_1 - n_2)A_{j1} + G^{'}(z_{o_2}, z_2)g_{i2}(\mu_2 n_1 - n_2)A_{j2}\right] \tag{12}$$

Introducing an intermediate point (z_c) in Eq.(9) and using the results from Reis (2013), we find a new expression for Eq.(9):

$$G(z_o, z) = \sum_{k=0}^{\infty} O_k(z_o - z_c)I_k(z - z_c) \tag{13}$$

where:

$$O_k(z) = \frac{(k-1)!}{z^k},\ \ for\ k > 1, \tag{14}$$

$$O_o(z) = -\log(z) \tag{15}$$

$$I_k(z) = \frac{z^k}{k!},\ \ for\ k > 0. \tag{16}$$

Doing the same procedures in Eq.(10), we find:

$$G^{'}(z_o, z) = \frac{\partial G(z_o, z)}{\partial z} = \frac{1}{(z - z_o)} = \sum_{k=1}^{\infty} O_k(z_o - z_c)I_{k-1}(z - z_c) \tag{17}$$

Complete proof of Eq.(13) and Eq.(17) can be found in Reis (2013). The key of FMM is presented by Eq.(13) and Eq.(17), because an auxiliary function was created with separation of the source point (z_o) and field point (z) by intermediate point (z_c) Braga (2012).

3.1 Multipole Expansion of the U kernel Integral - Moments

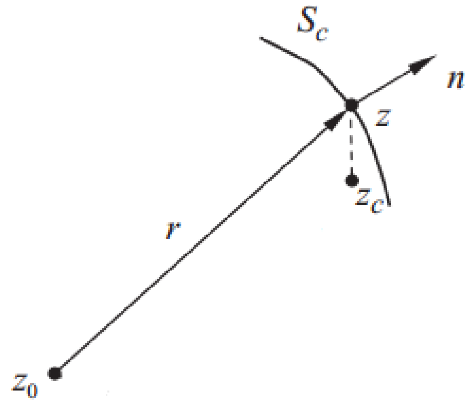

Figure 1: Mutilpole expansion around z - Liu (2009)

To present the multipole expansion, consider two intermediate points, (z_{c_1},z_{c_2}), near the field points (z_1,z_2). Consider the distances between $\mid z_1 - z_{c_1} \mid$ and $\mid z_2 - z_{c_2} \mid$ are less than $\mid z_{o_1} - z_{c_1} \mid$ and $\mid z_{o_2} - z_{c_2} \mid$. So, $\mid z_1 - z_{c_1} \mid \ll \mid z_{o_1} - z_{c_1} \mid$ and $\mid z_2 - z_{c_2} \mid \ll \mid z_{o_2} - z_{c_2} \mid$. Figure 1 illustrates the multipole expansion generically. Thus, using new auxiliary function $I_k(z)$ e $O_k(z)$ we have:

$$\begin{aligned}\int_\Gamma t_j U_{ij}(\mathbf{z_o}, \mathbf{z}) d\Gamma &= \int_\Gamma t_j (2Re\left[q_{i1}A_{j1}G(z_{o_1}, z_1) + q_{i2}A_{j2}G(z_{o_2}, z_2)\right]) d\Gamma \\ &= 2Re \int_\Gamma t_j q_{i1} A_{j1} G(z_{o_1}, z_1) d\Gamma + 2Re \int_\Gamma t_j q_{i2} A_{j2} G(z_{o_2}, z_2) d\Gamma \end{aligned} \quad (18)$$

To present the results of multipole expansion, we will work with the first integral on the right side of Eq.(18) first, after we present the same result for the second integral. So, using Eq.(13), we rewrite one part of Eq.(18) as:

$$2Re \int_\Gamma t_j [q_{i1} A_{j1} G(z_{o_1}, z_1)] d\Gamma = 2Re \int_\Gamma t_j q_{i1} A_{j1} \left(\sum_{k=0}^{\infty} O_{k_1}(z_{o_1} - z_{c_1}) I_{k_1}(z_1 - z_{c_1}) \right) d\Gamma \quad (19)$$

$$2Re \int_\Gamma t_j [q_{i1} A_{j1} G(z_{o_1}, z_1)] d\Gamma = 2Re \sum_{k=0}^{\infty} O_{k_1}(z_{o_1} - z_{c_1}) M_{k_1}(z_{c_1}) \quad (20)$$

where:

$$M_{k_1}(z_{c_1}) = \int_{S_c} t_j q_{i1} A_{j1} I_{k_1}(z_1 - z_{c_1}) dS \;\; k = 0, 1, 2, ... \quad (21)$$

Equation (21) is called *multipole expansion* and it can be readily evaluated, because there is no dependence with source point (z_o). So, for any position of (z_o) away from S_c, this term no longer needs to be recomputed, because it is computed just once. As a consequence, amount of operations, decreases. Similar results can be obtained for the second integral in Eq.(18):

$$2Re\int_{\Gamma} t_j[q_{i2}A_{j1}G(z_{o_2},z_2)]d\Gamma = 2Re\sum_{k=0}^{\infty} O_{k_2}(z_{o_2}-z_{c_2})M_{k_2}(z_{c_2}) \tag{22}$$

where:

$$M_{k_2}(z_{c_2}) = \int_{S_c} t_j q_{i2}A_{j2}I_{k_2}(z_2-z_{c_2})dS \;\; k=0,1,2,... \tag{23}$$

Equation (21) and Eq.(23) are known as *first moments* about (z_{c_1}) and (z_{c_2}). The same results can be expressed by Eq.(12):

$$\int_{\Gamma} u_j T_{ij}(\mathbf{z_o},\mathbf{z})d\Gamma = 2\Re\int_{\Gamma} u_j\left[G^{'}(z_{o_1},z_1)g_{i1}(\mu_1 n_1-n_2)A_{j1}\right]d\Gamma + \\ 2\Re\int_{\Gamma} u_j\left[G^{'}(z_{o_2},z_2)g_{i2}(\mu_2 n_1-n_2)A_{j2}\right]d\Gamma \tag{24}$$

The multipole expansions are:

$$2\Re\int_{\Gamma} u_j\left[G^{'}(z_{o_1},z_1)g_{i1}(\mu_1 n_1-n_2)A_{j1}\right]d\Gamma = 2\Re\sum_{k=0}^{\infty} O_k(z_{o_1}-z_{c_1})\tilde{M}_{k_1}(z_{c_1}) \tag{25}$$

where:

$$\tilde{M}_{k_1}(z_{c_1}) = \int_{S_c} u_j g_{i1}(\mu_1 n_1-n_2)A_{j1}I_{k_1-1}(z_1-z_{c_1})d\Gamma \;\; for \;\; k\geq 0 \tag{26}$$

and:

$$2\Re\int_{\Gamma} u_j\left[G^{'}(z_{o_2},z_2)g_{i2}(\mu_2 n_1-n_2)A_{j2}\right]d\Gamma = 2\Re\sum_{k=0}^{\infty} O_k(z_{o_2}-z_{c_2})\tilde{M}_{k_2}(z_{c_2}) \tag{27}$$

$$\tilde{M}_{k_2}(z_{c_2}) = \int_{S_c} u_j g_{i2}(\mu_1 n_1-n_2)A_{j2}I_{k_2-l}(z_2-z_{c_2})d\Gamma \;\; for \;\; k\geq 0 \tag{28}$$

where Eq.(26) and Eq.(28) are known as *second moments* about (z_{c_1}) and (z_{c_2}).

3.2 Moment to Moment Translation (M2M)

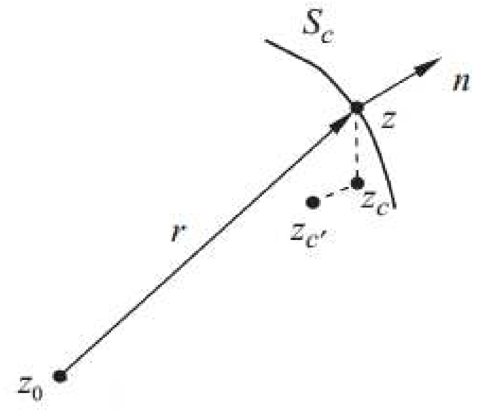

Figure 2: Translation z_c for $z_{c'}$ - Liu (2009)

Now, consider that the points (z_{c_1}) and (z_{c_2}) were moved to new positions $(z_{c'_1})$ and $(z_{c'2})$. This operation is known as *Moment to moment* (M2M) and represents a translation of points. Figure 2 shows this situation for generic case of M2M translation. So, to translate them, without recomputing Eq.(22) and Eq.(23), consider property below:

$$I_k(z_1 + z_2) = \sum_{l=0}^{k} I_{k-l}(z_1) I_l(z_2) = \sum_{l=0}^{k} I_l(z_1) I_{k-l}(z_2) \tag{29}$$

so:

$$M_{k_1}(z_{c'_1}) = \int_{S_c} t_j q_{i1} A_{j1} I_{k_1}(z_1 - z_{c'_1}) dS \tag{30}$$

$$M_{k_1}(z_{c'_1}) = \int_{S_c} t_j q_{i1} A_{j1} I_{k_1}[(z_1 - z_{c_1}) + (z_{c_1} - z_{c'_1})] dS \tag{31}$$

after some mathematical manipulations, we will find:

$$M_{k_1}(z_{c'_1}) = \sum_{l=0}^{k} I_{k_1 - l}(z_{c_1} - z_{c'_1}) M_{l_1}(z_{c_1}) \ \ k \geq 0 \tag{32}$$

where $M_{l_1}(z_{c_1})$ is given by:

$$M_{l_1}(z_{c_1}) = \int_{S_c} t_j q_{i1} A_{j1} I_{l_1}(z_1 - z_{c_1}) dS \tag{33}$$

Doing same steps for Eq.(30), we found:

$$M_{k_2}(z_{c'_2}) = \sum_{l=0}^{k} I_{k_2-l}(z_{c_2} - z_{c'_2}) M_{l_2}(z_{c_2}) \;\; for \;\; k \geq 0 \tag{34}$$

where $M_{l_2}(z_{c_2})$ is given by:

$$M_{l_2}(z_{c_2}) = \int_{S_c} t_j q_{i2} A_{j2} I_{l_2}(z_2 - z_{c_2}) dS \tag{35}$$

where Eq.(32) and Eq.(34) are known as *M2M tranlastion*.The same results can be written for Eq.(26) and Eq.(28):

$$\tilde{M}_{k_1}(z_{c'_1}) = \sum_{l=0}^{k} I_{k_1-l}(z_{c_1} - z_{c'_1}) \tilde{M}_{l_1}(z_{c_1}) \;\; for \;\; k \geq 1 \tag{36}$$

where $\tilde{M}_{l_1}(z_{c_1})$ is given by:

$$\tilde{M}_{l_1}(z_{c_1}) = \int_{S_c} t_j g_{i1}(\mu_1 n_1 - n_2) A_{j1} I_{l_1-l}(z_1 - z_{c_1}) dS \tag{37}$$

and:

$$\tilde{M}_{k_2}(z_{c'_2}) = \sum_{l=0}^{k} I_{k_2-l}(z_{c_2} - z_{c'_2}) \tilde{M}_{l_2}(z_{c_2}) \;\; fork \;\; \geq 1 \tag{38}$$

being $\tilde{M}_{l_2}(z_{c_2})$ is given by:

$$\tilde{M}_{l_2}(z_{c_2}) = \int_{S_c} t_j g_{i2}(\mu_2 n_1 - n_2) A_{j2} I_{l_2-l}(z_2 - z_{c_2}) dS \tag{39}$$

3.3 Local Expansion and Moment to Local Translation (M2L)

Now, we do more two operations, called *Local Expansion* and *Moment-to-Local Translation* (M2L). In this situation, two points, (z_{L_1}) and (z_{L_2}), are introduced next to source points (z_{o1}) and (z_{o2}), as presented in Figure 3. Consider the approximations ($| \; z_{o_1} - z_{L_1} \; | \ll | \; z_1 - z_{L_1} \; |$) and ($| \; z_{o_2} - z_{L_2} \; | \ll | \; z_2 - z_{L_2} \; |$). From Eq.(19), the local expansion can be represented by:

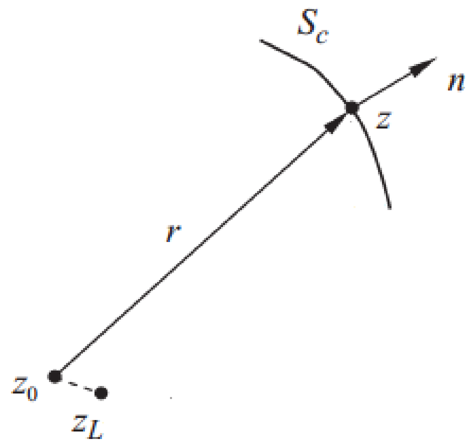

Figure 3: Local expansion around z_L - Liu (2009)

$$2Re \int_\Gamma t_j[q_{i1}A_{j1}G(z_{o_1}, z_1)]d\Gamma = 2Re \sum_{k=0}^{\infty} O_{k_1}[(z_{L_1} - z_{c_1}) + (z_{o_1} - z_{c_1})]M_{k_1}(z_{c_1}) \quad (40)$$

Considering propriety below:

$$O_k(z_1 + z_2) = \sum_{l=0}^{\infty}(-1)^l O_{k+l}(z_1)I_l(z_2) \;\; for \; |z_2| < |z_1| \quad (41)$$

Equation (19) is written as:

$$2Re \int_\Gamma t_j[q_{i1}A_{j1}G(z_{o_1}, z_1)]d\Gamma = 2Re \left[\sum_{l=0}^{\infty}(-1)^l O_{k_1+l_1}(z_{L_1} - z_{c_1})I_{l_1}(z_{o_1} - z_{c_1})\right] M_{k_1}(z_{c_1}) \quad (42)$$

After some manipulations, we have following results:

$$2Re \int_\Gamma t_j[q_{i1}A_{j1}G(z_{o_1}, z_1)]d\Gamma = 2Re \left[\sum_{l=0}^{\infty} L_{k_1}(z_{L_1})I_{l_1}(z_{o_1} - z_{c_1})\right] \quad (43)$$

where:

$$L_{k_1}(z_{L_1}) = (-1)^k \left[\sum_{k=0}^{\infty} O_{k_1+l_1}(z_{L_1} - z_{c_1})I_{l_1}(z_{o_1} - z_{c_1})\right] M_{k_1}(z_{c_1}) \;\; for \;\; l \geq 1 \quad (44)$$

Equation (43) is called *local expansion* and Eq.(44) is *Moment-to-local Translation* (M2L). Finally, same results can be obtained for the following equation:

$$2Re \int_\Gamma t_j[q_{i2}A_{j2}G(z_{o_1}, z_2)]d\Gamma = 2Re \left[\sum_{l=0}^{\infty} L_{k_2}(z_{L_2})I_{l_2}(z_{o_2} - z_{c_2})\right] \quad (45)$$

$$L_{k_2}(z_{L_2}) = (-1)^k \left[\sum_{k=0}^{\infty} O_{k_2+l_2}(z_{L_2} - z_{c_2}) I_{l_2}(z_{o_2} - z_{c_2}) \right] M_{k_2}(z_{c_2}) \tag{46}$$

Doing the same procedures for first integral of Eq.(24), we have:

$$2\Re \int_{\Gamma} t_j [g_{i1}(\mu_1 n_1 - n_2) A_{j1} G(z_{o_1}, z_1)] d\Gamma = 2\Re \left[\sum_{l=0}^{\infty} \tilde{L}_{k_1}(z_{L_1}) I_{l_1}(z_{o_1} - z_{c_1}) \right] \tag{47}$$

where:

$$\tilde{L}_{k_1}(z_{L_1}) = (-1)^k \left[\sum_{k=0}^{\infty} O_{k_1+l_1}(z_{L_1} - z_{c_1}) I_{l_1-1}(z_{o_1} - z_{c_1}) \right] \tilde{M}_{k_1}(z_{c_1}) \;\; for \;\; l \geq 1 \tag{48}$$

for the second integral of Eq.(24), we have:

$$2\Re \int_{\Gamma} t_j [g_{i1}(\mu_2 n_1 - n_2) A_{j2} G(z_{o_2}, z_2)] d\Gamma = 2\Re \left[\sum_{l=0}^{\infty} \tilde{L}_{k_2}(z_{L_2}) I_{l_2}(z_{o_2} - z_{c_2}) \right] \tag{49}$$

$$\tilde{L}_{k_2}(z_{L_2}) = (-1)^k \left[\sum_{k=0}^{\infty} O_{k_2+l_2}(z_{L_2} - z_{c_2}) I_{l_2-1}(z_{o_2} - z_{c_2}) \right] \tilde{M}_{k_1}(z_{c_2}) \;\; for \;\; l \geq 1 \tag{50}$$

3.4 Local to local translations

Finally, the last translation is known as *local to local* (L2L), and represents a translation of points z_{L_1} and z_{L_2} to $z_{L'_1}$ and $z_{L'_2}$, respectively. Thus, equation found is:

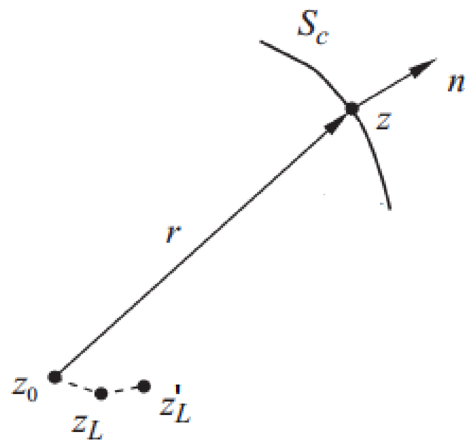

Figure 4: Translation z_L for $z_{L'}$ - Liu (2009)

$$2Re \int_{\Gamma} t_j [q_{i1} A_{j1} G(z_{o_1}, z_1)] d\Gamma = 2Re \left[\sum_{l=0}^{\infty} L_{k_1}(z_{L_1}) I_{l_1}((z_{o_1} - z_{L'_1}) + (z_{L'_1} - z_L)) \right] \tag{51}$$

$$2Re\int_{\Gamma} t_j[q_{i1}A_{j1}G(z_{o1},z_1)]d\Gamma = 2Re\sum_{l=0}^{\infty} L_{k_1}(z_{L'_1})I_{p_1}(z_{o_1}-z_{L'_1}) \tag{52}$$

being the term $L_{k_1}(z_{L'_1})$ given by:

$$L_{k_1}(z_{L'_1}) = \sum_{k=0}^{p-l} I_{k_1-l_1}(z_{L'_1}-z_L)L_{l+k}(z_{l_1}) \tag{53}$$

where Eq.(53) is *Local-to-Local translation* (L2L). Following same steps, we obtain:

$$2Re\int_{\Gamma} t_j[q_{i2}A_{j2}G(z_{o_1},z_2)]d\Gamma = 2Re\sum_{l=0}^{\infty} L_{k_2}(z_{L'_2})I_{p_2}(z_{o_2}-z_{L'_2}) \tag{54}$$

$$L_{k_2}(z_{L'_2}) = \sum_{k=0}^{p-l} I_{k_2-l_2}(z_{L'_2}-z_L)L_{l_2+k_2}(z_{L_2}) \tag{55}$$

4 Fast multipole algorithm and its characteristics

In this section, we will present some characteristics of FMM and how the operations described previously are used. First of all, the boundary of the problem can be discretized by constant elements, linear elements or quadratic elements. In this article, we discretized the problems with *N* constant elements, after *tree structure* is used, to group elements that are near and far from the source point.

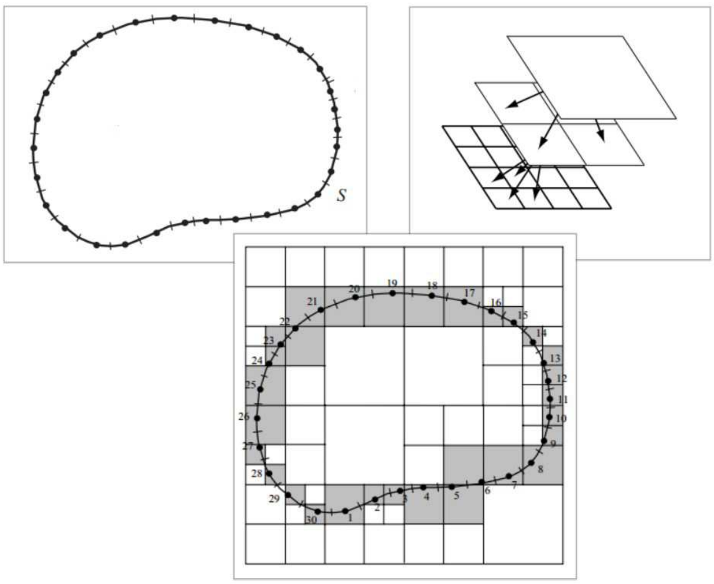

Figure 5: Boundary subdivided by square - Liu (2009)

The first step is to circumscribe the entire boundary by a square *cell*, being it called cell of level 0. The next level is created by dividing the cell of level 0 into four equal cells. This is the level 1 and its cells are considered *child cells* of the *parent cell* of level 0. This nomenclature is related to interdependence created between these two levels. The edge length of these cells is calculated by $L/2^l$, being *L* the length of the cell at level 0 and *l* is the level where the cells are Liu (2009). We continue dividing the cells until we reach a specific number of elements in a child cell that should not exceed a predetermined number (denoted by *M*) of elements per cell Liu (2009). In Figure 5 we have an example of subdivision with one element per cell. An element belongs to a cell if its center is inside the cell. The cell that was element called *leaf cell*, because it does not have a child cell. Nishimura (2002) shows that the numbers of leaves are estimated as $O(N/M)$, the numbers of other cells are $O(N/M)X((1/4)+(1/4)^2$ $+ ...) \simeq O(N/M)$ and the number of levels are $O(log(N/M))$.

Now, we will present how the operations used are described. First of all, we compute the moments on all cells that are in level $l \geq 2$, with a certain number of *p* terms in Taylor Series. First operation, we use is *multipole expansion*, to transfer position of node of the element to the centroid of leaf cell (z_c). After, we move the centroid of the leaf cell to the centroid of its father cell. To do this transfer, we use $M2M$. We will continue this process until we reach level 2, as presented above, carrying position of these centroids with operation $M2M$. This process is known as *upward*. Figure 6 represents *upward*. In this step, moments are computed for each new iteration, because there is an integral of the kernel and estimation of the boundary solutions, Liu (2009). The complexity of this level is given as $O(pN) + O(p^2(N/M))$, where $O(pN)$ operations is to compute the multipole expansion and the $O(p^2(N/M))$ operations to compute M2M Nishimura (2002).

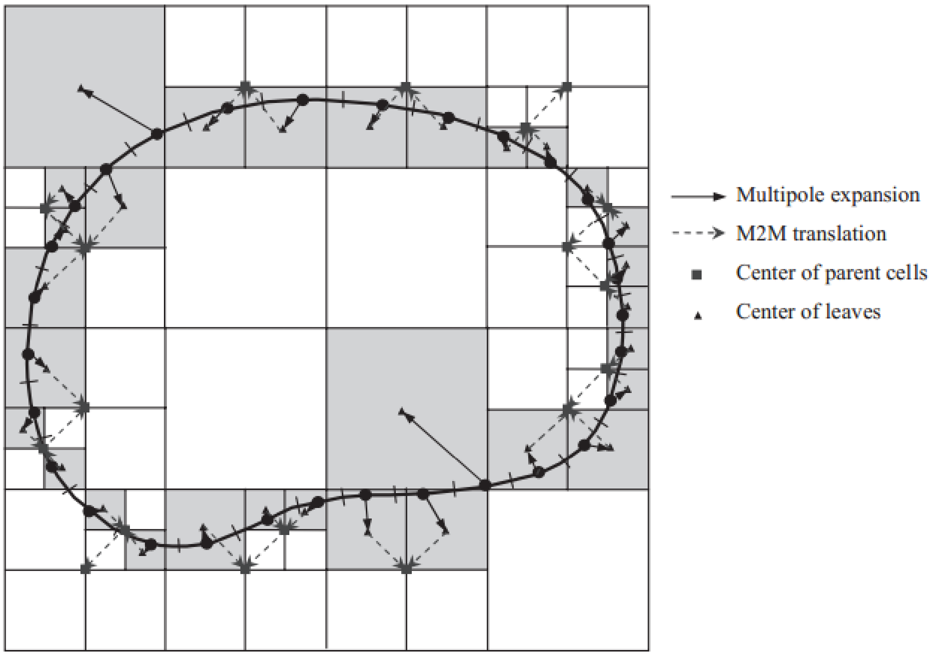

Figure 6: Upward process - Liu (2009)

Once we reach the level 2, we use the operations $M2L$, *L2L* and *local expansion* to describe *downward* process. Before using these operations, we use subdivision created by tree hierarchy to qualify cells that are *adjacent*, *well separated* and *far* from the leaf cell that contains the element with source point. The *adjacent cells* are those that have, at least, one vertex in common at the same level. For leaves cells at different levels, they are *adjacent* if their parent cells have one vertex in common. For cells considered *well separated*, we should look at the relationship between their parent cells, because they are not adjacent at the same level. Thus, if their parent cells are adjacent at level $l-1$, they are considered *well separated*. As an example, in Figure 7, the cells in the *interaction list* are *well separated* from cell C. By the end, a cell is considered *far* if it does not have adjacent parent cells.

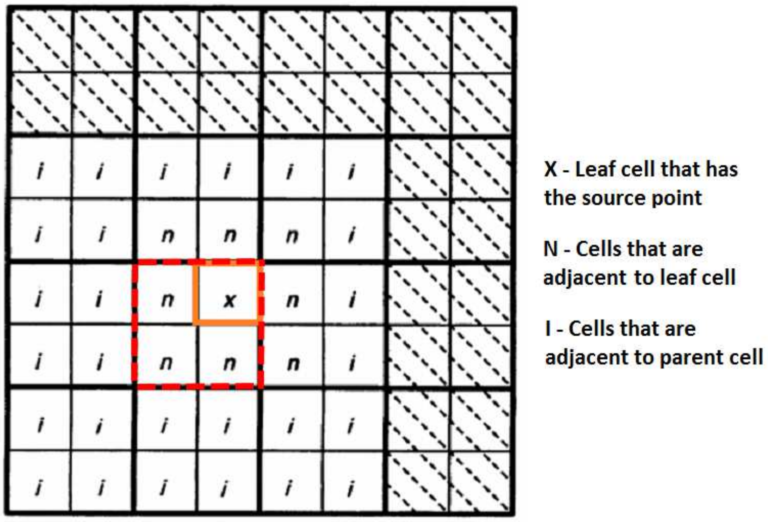

Figure 7: Relation between the cells - Liu (2009)

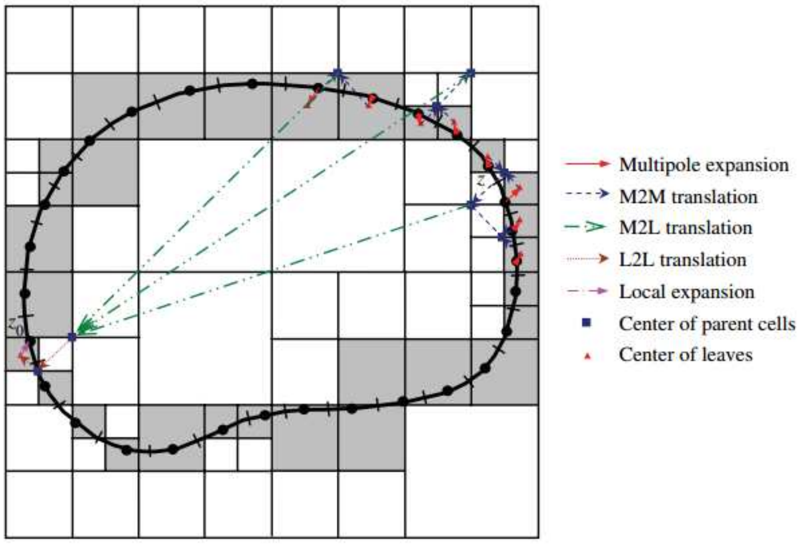

Figure 8: Upward and downward process - Nishimura (2002)

After this classification, we start *downward* process from level 2, computing local expansion coefficients on all cells. These coefficients are the contribution of cells that are in the interaction list and that are far. To compute these terms, we use $M2L$ translation and $L2L$ translation. First translation is used for cells in an interaction list (well separated cells) and second translation is used for far cells. The complexity of this process is $O(p^2(N/M))$, where the order of M2L and L2L operations are $O(p^2)$ each one Nishimura (2002). Figure 8 shows how all operations are used to do the FMM. Finally, the next step is evaluating the integrals of BEM. As an example, consider Eq.(18):

$$\begin{aligned}
&\int_\Gamma t_j U_{ij}(\mathbf{z_o}, \mathbf{z}) d\Gamma = 2\Re \int_\Gamma t_j q_{i1} A_{j1} G(z_{1o}, z_1) d\Gamma + \\
&2\Re \int_\Gamma t_j q_{i2} A_{j2} G(z_{2o}, z_2) d\Gamma = 2\Re \int_{\Gamma_{Near}} t_j q_{i1} A_{j1} G(z_{1o}, z_1) d\Gamma + \\
&2\Re \int_{\Gamma_{Far}} t_j q_{i1} A_{j1} G(z_{1o}, z_1) d\Gamma + 2Re \int_{\Gamma_{Near}} t_j q_{i2} A_{j2} G(z_{2o}, z_2) d\Gamma + \\
&2\Re \int_{\Gamma_{Far}} t_j q_{i2} A_{j2} G(z_{2o}, z_2) d\Gamma
\end{aligned} \tag{56}$$

where integral in Eq.(56) is decomposed into two parts, one with (Γ_{Near}) boundary and the other with (Γ_{Far}) boundary. The integrals with (Γ_{Near}) boundaries are computed by conventional BEM and the integrals with(Γ_{Far}) boundaries are computed by fast BEM with an iterative solver. In this part, the iterative solver will update the unknown solution vector λ in the system $\mathbf{A}\lambda = \mathbf{b}$. This process continues until the solution of λ converges within the given tolerance. When a new iterative process restarts, the beginning is the upward passage.

5 Result

In this section we compare memory used to solve an anisotropic plane elasticity problem with different number of DOFs. The problem analyzed was a square plate with 16, 64 and 100 holes. The plate has 1 m^2 and the holes have an area of 12.47 % of the plate area. An edge is fixed while another is under tension (see Figure 9). For each situation with different numbers of holes, we use 1, 10 and 20 elements per cells. The number of elements on each plate edge and for each hole is 8. We used 8 terms in Taylor series. The tolerance used in GMRES was 10^{-6}. The properties of the plate is shown in the Tables 1 and 2.

Table 2: Properties of composite material

Layer	$E_1(GPa)$	$E_2(GPa)$	$G_{12}(GPa)$	ν_{12}	θ
1	2.2	4.4	0.7692	0.4286	-15^o
2	2.2	4.4	0.7692	0.4286	25^o

With the results obtained, we notice that increase of DOFs requires more time and memory used to solve the problem. It was clearly expected, because the number of DOFs represents the size of the problem. On the other hand, the difference of the number inside the cells did not show many differences between them. So, it made it possible not to raise the performance of the method changing the number of nodes in the cells. Thus, it will be necessary to analyze otherproblems more complex to observe effects of nodes inside cells.

Table 3: Solution of the problem for 1 Element per cell

1 Element per cell			
	Nodes	Time (s)	Memory (Mbytes)
4X4	160	133	664
8X8	544	1277	694
10x10	832	2242	717

Table 4: Solution of the problem for 10 Elements per cell

10 Elements per cell			
	Nodes	Time (s)	Memory (Mbytes)
4X4	160	269	701
8X8	544	1091	710
10x10	832	1630	734

Table 5: Solution of the problem for 20 Elements per cell

20 Elements per cell			
	Nodes	Time (s)	Memory (Mbytes)
4X4	160	244	706
8X8	544	988s	711
10x10	832	2273	724

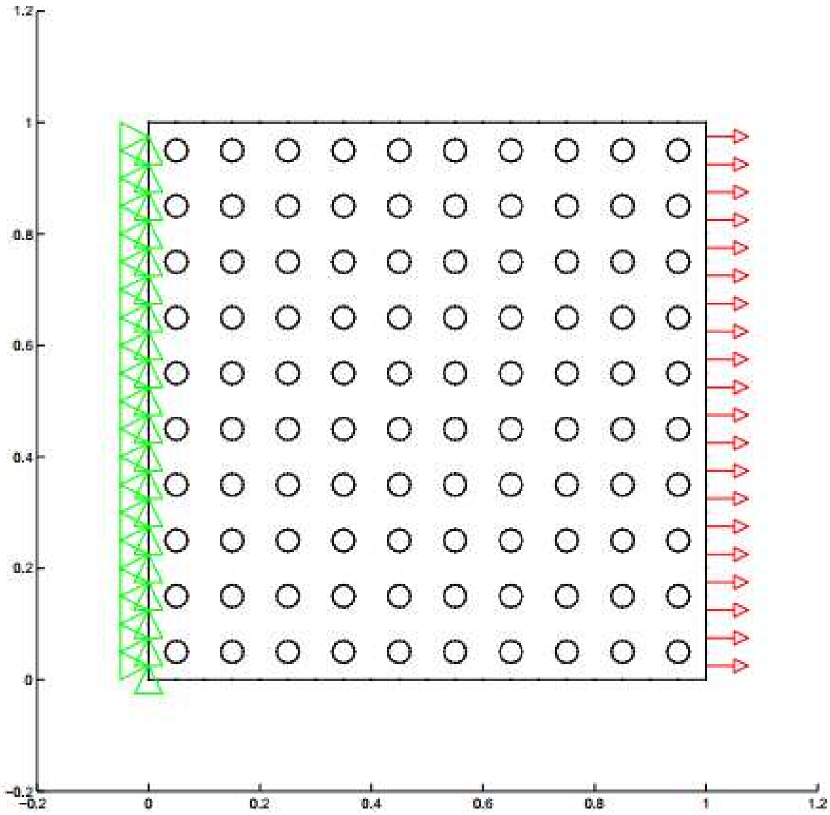

Figure 9: Mesh of the model

5.1 Conclusion

The idea of this paper was to present the formulation of fast BEM to solve large scale problems for anisotropic plane elasticity for different number of elements per cell. We could observe that the consumption of memory and time increase if the number of DOFs rise. However, the results can not accurately show the difference between time and memory of the simulation for different number of elements per cell. It was expected to find more information about how fast multipole formulation works with this kind of difference. This information is important because it shows how we can simulate problems with more DOFs efficiently. So, to study this kind of behavior maybe it would be necessary to increase the number of DOFs of the problem to see if it is possible to find a huge difference between time and memory for different number of elements per cell.

Bibliography

E.L. Albuquerque. *Numerical analysis of dynamic anisotropic problems using the boundary element method*. PhD thesis, Unicamp, Dept. Mec. Comput., July 2001. In Portuguese.

L. M. Braga. The fast multipole method for potencial problems. Master's thesis, Universidade de Brasília, Dept. Eng. Mecânica, agosto 2012. In Portuguese.

L.F. Greengard and V. Rokhlin. A fast algorithm for particle simulations. *J.Comp Phys*, 73: 325–348, 1987.

Buchau A. Groh F. Rucker W.M. Hafla, W. Fast multipole method applied to volume integral equation method. *Advances in Radio Science*, 3:195–198, 2005.

Nishimura N. Otani Y. Liu, Y.J. Large-scale modeling of carbon-nanotube composites by a fast multipole boundary element method. *Computational Materials Science*, 34:173–187, 2005.

Y. Liu. A fast multipole boundary element method for 2d multi-domain elastostatic problems based on a dual bie formulation. *Computational Mechanics*, 42:761–733, 2008.

Y. Liu. *Multipole boundary element method - Theory and Applications in Engineering*. Cambridge. 2009.

N. Nishimura. Fast multipole accelerated boundary integral equation methods. *Applied Mechanics Reviews*, 54:299–324, 2002.

Napier J.A.L. Peirce, A.P. A spectral multipole method for efficient solution of large-scale boundary element models in elastostatics. *Int. J. Numer. Methods*, 38:409–434, 1995.

Power H. Popov, V. An o(n) taylor series multipole boundary element method for three-dimensional elasticity problems. *Engineering Analysis with Boundary Elements*, 25:718, 2001.

Albuquerque E.L. Anflor C.M. Reis, A. Series expansions of anisotropic plane elasticity fundamental solutions. In *International Conference on Boundary Element and Meshless Techniques*, 2013.

P. Sollero. *Fracture mechanics analysis of anisotropic laminatesby the boundary element method*. PhD thesis, Wessex Institute of Technology, 1994.

Yao Z.H. Wang, H.T. A new fast multipole boundary element method for large scale analysis of mechanical properties in 3d particle-reinforced composites. *Computer Modeling in Engineering and Sciences*, 7:85–95, 2005.

Yao Z.H. Wang, P.B. Application of a new fast multipole bem for simulation of 2d elastic solid with large number of inclusions. *Acta Mechanica Sinica*, 20:613–622, 2004.

Yao Z.H. Wang, P.B. Fast multipole dbem analysis of fatigue crack growth. *Computational Mechanics*, 38:223–233, 2006.

Nishimura N. Kobayashi S. Yoshida, K. pplication of new fast multipole boundary integral equation method to crack problems in 3d. *Engineering Analysis with Boundary Elements*, 50:239–247, 2001a.

Nishimura N. Kobayashi S. Yoshida, K. Application of fast multipole galerkin boundary integral equation method to elastostatic crack problems in 3d. *International Journal for Numerical Methods in Engineering*, 50:525–547, 2001b.

Xia Y. Chunjian S. Zejun C., Hong X. Taylor series multipole boundary element-mathematical programming method for 3d multi-bodies elastic contact problems. *International Journal for Numerical Methods in Engineering*, 83:135–173, 2010.